

# Mechanistic Insights into Oxidative Decomposition of *exo*-Tetrahydrodicyclopentadiene

Sun Hee Park,<sup>†,‡,#</sup> Cheong Hoon Kwon,<sup>†,#</sup> Joongyeon Kim,<sup>†</sup> Jeong Sik Han,<sup>§</sup> Byung Hun Jeong,<sup>§</sup> Hogyu Han,<sup>\*,||</sup> and Sung Hyun Kim<sup>\*,†</sup>

<sup>†</sup>Department of Chemical & Biological Engineering, Korea University, Seoul 136-701, Korea

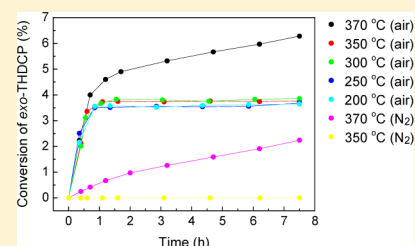
<sup>‡</sup>Korea Atomic Energy Research Institute, 150 Deokjin-dong, Yuseong-gu, Daejeon 305-353, Korea

<sup>§</sup>Agency for Defense Development, 111 Sunam-dong, Yuseong-gu, Daejeon 305-152, Korea

<sup>||</sup>Department of Chemistry, Korea University, Seoul 136-701, Korea

## S Supporting Information

**ABSTRACT:** We investigated the decomposition of *exo*-tetrahydrodicyclopentadiene (*exo*-THDCP, C<sub>10</sub>H<sub>16</sub>) in the absence and presence of O<sub>2</sub> at various temperatures. It was found that conversion of *exo*-THDCP was faster in the presence of O<sub>2</sub> as compared to in its absence. The O<sub>2</sub>-induced increase in the conversion of *exo*-THDCP was hardly affected by variations in temperature. In addition, the O<sub>2</sub>-induced increase in the rate of C<sub>10</sub> product formation was higher than those of <C<sub>10</sub> and >C<sub>10</sub>. We proposed the mechanism for the oxidative decomposition of *exo*-THDCP, which occurs independently of its thermal decomposition and induces distinct product formation near and below its thermal decomposition starting temperature.



## 1. INTRODUCTION

Fuel is a primary coolant for the hydraulics, control systems, and engines in aircraft.<sup>1–4</sup> When fuel is subjected to high temperatures, it undergoes thermal and oxidative decomposition to form gum and coke, which cause many problems such as fouling and plugging. Thermal and oxidative decomposition of fuel need to be lowered for the proper functioning of the engine and subsystem.

*exo*-Tetrahydrodicyclopentadiene (*exo*-THDCP, C<sub>10</sub>H<sub>16</sub>) is a synthetic liquid fuel with a multicyclic structure.<sup>5–28</sup> *exo*-THDCP has attracted significant attention due to its high energy density, which is greater than those of conventional kerosene-based fuels and renders it suitable for use in volume-limited aircraft.

Several studies on the oxidative decomposition of *exo*-THDCP using experimental and computational methods have been reported.<sup>15,20,21,23,24</sup> Formation of hydroperoxide upon oxidative decomposition of *exo*-THDCP was observed by ultraviolet–visible spectroscopy.<sup>15</sup> The energies of radicals formed upon H abstraction of *exo*-THDCP were calculated using computational methods, and its oxidative decomposition products were predicted.<sup>20,21,23,24</sup> However, a mechanistic study on the oxidative decomposition of *exo*-THDCP in the liquid phase below its thermal decomposition starting temperature has not been conducted yet.

Here, we report the study on the decomposition of *exo*-THDCP in the absence and presence of O<sub>2</sub> at various temperatures. It was found that the oxidative decomposition of *exo*-THDCP occurred independently of its thermal decomposition. We proposed the mechanism for the oxidative decomposition of *exo*-THDCP, which explains distinct product

formation thereupon near and below its thermal decomposition starting temperature.

## 2. EXPERIMENTAL SECTION

**2.1. Experimental Methods.** Decomposition of *exo*-THDCP (100 mL) in the absence and presence of O<sub>2</sub> at various temperatures was carried out in a batch reactor (160 mL) as reported previously.<sup>26</sup> A quartz flask was inserted inside a stainless steel reactor, and a quartz plate was placed on the inside of the stainless steel reactor cover. Quartz was used to block any possible catalytic role of stainless steel or other metals. The pressure inside the reactor was set at 40 bar of N<sub>2</sub> or air, which is higher than the critical pressure (38 bar) of *exo*-THDCP.<sup>11</sup>

Hydrocarbon compounds and the hydrogen molecule were analyzed on gas chromatography–mass spectrometry (GC–MS, Agilent 7890A, 5975C), GC–flame ionization detection (GC–FID, Agilent 7890A), and GC–thermal conductivity detection (GC–TCD, Agilent 7890A) systems as reported previously.<sup>26</sup>

Conversion of *exo*-THDCP and the composition of the product were measured as reported previously.<sup>26</sup> Conversion of *exo*-THDCP is defined as

$$\text{conversion of } \textit{exo}\text{-THDCP (\%)} = \frac{C_0 - C_t}{C_0} \times 100$$

Received: May 14, 2013

Revised: June 28, 2013

Published: July 1, 2013

where  $C_0$  and  $C_t$  are the concentrations (wt %) of *exo*-THDCP at the initial and indicated times, respectively.  $C_t$  was determined by GC analysis as described above. The composition of the product is defined as the ratio (wt %/wt %) of  $C_n$  to all compounds, where  $C_n$  indicates all compounds with  $n$  number of carbons, unless otherwise noted. Standard deviations of product compositions were smaller than 0.01%.<sup>26</sup>

## 2.2. Molecular and Quantum Mechanics Calculations.

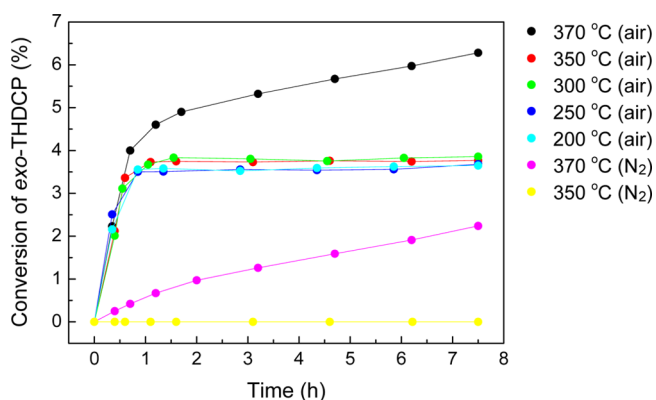
The geometry optimized structures and energies of *exo*-THDCP and its oxidatively decomposed intermediates and products were calculated using the molecular mechanics (MM3), parameterized model (PM3), and Austin model (AM1) methods in the MOPAC program (Fujitsu CAChe 7.7).<sup>29–33</sup> The geometry optimized structures thus obtained were then employed to calculate the energy changes for bond breaking and forming processes. Such energy changes were used to determine the possible reaction pathways as reported previously.<sup>28</sup>

## 3. RESULTS AND DISCUSSION

### 3.1. Oxidative Decomposition of *exo*-THDCP.

Decomposition of hydrocarbon fuels in the absence and presence of  $O_2$  is affected by temperature and pressure.<sup>26</sup> We found that conversion of *exo*-THDCP and the product composition were hardly affected by variations in the pressure of  $N_2$  (28–40 bar), whereas they were strongly affected by those of  $O_2$  (12–0 bar) at the total pressure of 40 bar and 200–370 °C (data not shown). The ratio of gaseous products such as hydrogen gas, methane, ethane, ethene, propane, propene, and butane to all compounds was  $\sim 0.1\%$  regardless of whether  $O_2$  was present or not. Therefore, we analyzed the compositions of liquid products to measure the decomposition of *exo*-THDCP in the absence and presence of  $O_2$  at various temperatures. The reaction pressure was set at 40 bar of  $N_2$  or air, which mimics a real system, where fuels are subjected to pressures higher than 35 bar.<sup>3</sup>

Conversions of *exo*-THDCP in the absence and presence of  $O_2$  at 200–370 °C for 7.5 h are shown in Figure 1. At 200–350

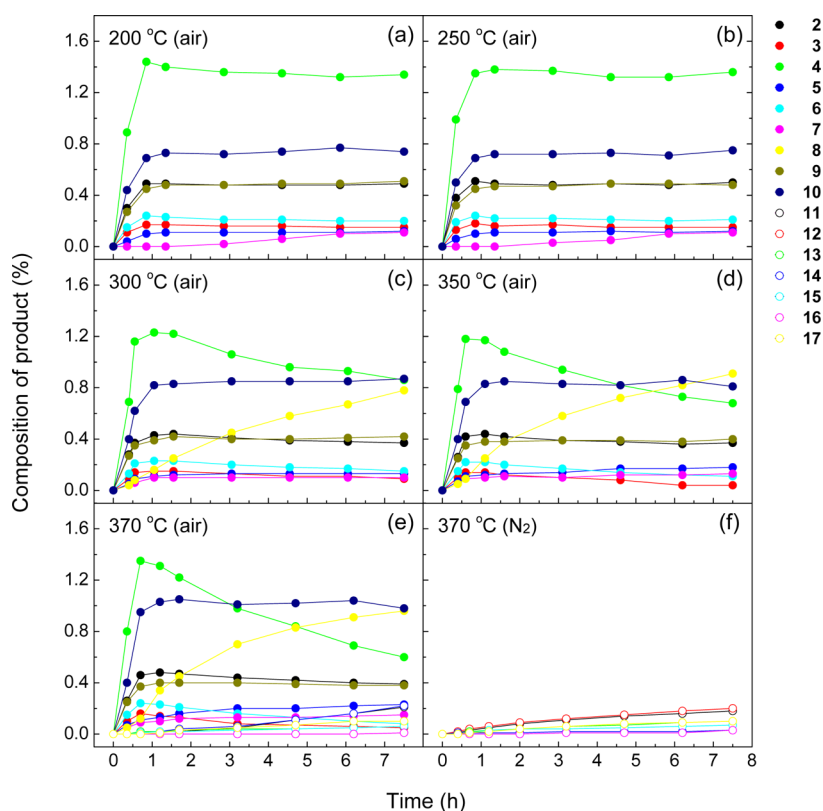


**Figure 1.** Conversions of *exo*-THDCP at 200–370 °C and 40 bar of air or  $N_2$  for 7.5 h.

°C, conversions of *exo*-THDCP were 0.0% in the absence of  $O_2$ , whereas they reached 3.8% within 1 h, which lasted until the end of the reaction in the presence of  $O_2$ . At 370 °C, conversion of *exo*-THDCP steadily increased to 2.2% over 7.5 h in the absence of  $O_2$ , whereas it reached 3.8% within 1 h and steadily increased to 6.3% over 7.5 h in the presence of  $O_2$ . Thus, at 200–370 °C, conversion of *exo*-THDCP was faster in

the presence of  $O_2$  compared to in its absence. Conversion of *exo*-THDCP in the presence of  $O_2$  at 370 °C appeared to be the simple sum of its conversions in the presence of  $O_2$  at 200–350 °C and in the absence of  $O_2$  at 370 °C. Note that the  $O_2$ -induced increases in the conversion of *exo*-THDCP were nearly identical at 200–350 °C. Thus, the  $O_2$ -induced increase in the conversion of *exo*-THDCP was hardly affected by variations in temperature (200–370 °C). Unlike the oxidative decomposition of *exo*-THDCP, however, its thermal decomposition was faster at the higher temperature (see Figure 1, magenta and yellow).

Compositions of products formed from *exo*-THDCP in the absence and presence of  $O_2$  at 200–370 °C for 7.5 h are shown in Figure 2 and Table 1. At 200–350 °C, where products were not formed from *exo*-THDCP in the absence of  $O_2$ , most of the products formed in the presence of  $O_2$  were  $C_{10}$  compounds (Figure 2a–d). At 200 and 250 °C, the order of the product formation rate in the presence of  $O_2$  was  $4 > 10 > 2 > 9 > 6 > 3 > 5 > 7$ . Their ratios to all compounds reached 1.44%, 0.69%, 0.49%, 0.45%, 0.24%, 0.17%, 0.10%, and 0.00% at 200 °C, and 1.35%, 0.69%, 0.51%, 0.45%, 0.24%, 0.18%, 0.10%, and 0.00% at 250 °C, respectively, within 1 h, which lasted until the end of the reaction, during which conversion of *exo*-THDCP was not changed. At 300 and 350 °C, the order of the product formation rate in the presence of  $O_2$  was  $4 > 10 > 2 > 9 > 6 > 8 > 3 > 5 > 7$ . Their ratios to all compounds reached 1.23%, 0.82%, 0.43%, 0.39%, 0.23%, 0.16%, 0.15%, 0.11%, and 0.10% at 300 °C, and 1.17%, 0.83%, 0.44%, 0.38%, 0.22%, 0.25%, 0.14%, 0.12%, and 0.10% at 350 °C, respectively, within 1 h, which lasted until the end of the reaction except for 4, 2, and 8. After 1 h, the ratios of 4 and 2 to all compounds gradually decreased, whereas that of 8 concomitantly increased while conversion of *exo*-THDCP was not changed. It seems that products 4 and 2 are further converted into 8. At 370 °C, most of the products formed in both the absence and presence of  $O_2$  were  $C_{10}$  compounds, although the products were somewhat different depending on whether  $O_2$  was present or not (Figure 2e and f). At 370 °C, the order of the product formation rate in the presence of  $O_2$  was  $4 > 10 > 2 > 9 > 8 > 6 > 3 > 5 > 7 \gg 12 > 11 > 13 > 14 > 15 > 16 > 17 > 16$ . At 370 °C, the order of the product formation rate in the absence of  $O_2$  was  $12 > 11 > 13 > 15 > 17 > 14 > 16$ . Thus, the products from *exo*-THDCP in the presence of  $O_2$  at 370 °C appeared to be the simple sum of those in the presence of  $O_2$  at 200–350 °C and in the absence of  $O_2$  at 370 °C. It seems that the products from *exo*-THDCP in the presence of  $O_2$  at 370 °C are composed of the oxidative (2–10) and thermal (11–17) decomposition products, which are formed from *exo*-THDCP independently of each other. The ratios of oxidative decomposition products 4, 10, 2, 9, 8, 6, 3, 5, and 7 to all compounds reached 1.31%, 1.03%, 0.48%, 0.40%, 0.34%, 0.23%, 0.14%, 0.13%, and 0.10%, respectively, within 1 h at 370 °C, which lasted until the end of the reaction except for 4, 2, and 8. After 1 h, the ratios of 4 and 2 to all compounds gradually decreased, whereas that of 8 concomitantly increased while conversion of *exo*-THDCP was not changed. It seems that products 4 and 2 are further converted into 8. The ratios of thermal decomposition products 12, 11, 13–15, 17, and 16 to all compounds almost linearly increased until 7.5 h regardless of whether  $O_2$  was present or not at 370 °C. Their ratios to all compounds in the presence (absence) of  $O_2$  were 0.02%, 0.02%, 0.02%, 0.02%, 0.01%, and 0.00% (0.06%, 0.05%, 0.03%, 0.01%, 0.03%, 0.02%, and 0.00%) for 1 h, and 0.21%, 0.20%, 0.06%, 0.05%, 0.06%, 0.10%, and 0.01% (0.20%, 0.18%,



**Figure 2.** Compositions of products formed upon decomposition of *exo*-THDCP at 200–370 °C and 40 bar of air or N<sub>2</sub> for 7.5 h. See Table 1 for the names, structures, and formulas of products 2–17. See also Figure S1 and Tables S1–S3 of the Supporting Information. Oxidative (2–10) and thermal (11–17) decomposition products (see the detailed discussion in 3.1) are indicated by solid and open circles, respectively.

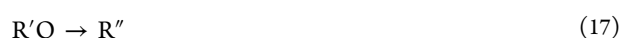
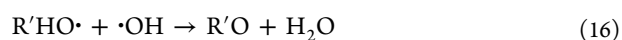
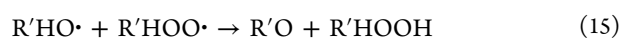
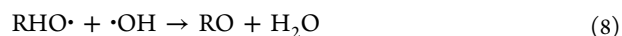
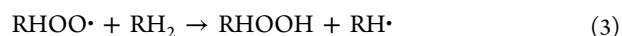
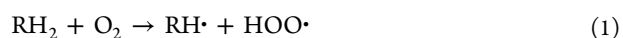
0.10%, 0.03%, 0.07%, 0.10%, and 0.03%) for 7.5 h, respectively, at 370 °C. Note that at 200–370 °C, most of the oxidative decomposition products from *exo*-THDCP were C<sub>10</sub> compounds. Thus, the O<sub>2</sub>-induced increase in the rate of C<sub>10</sub> product formation was higher than those of <C<sub>10</sub> and >C<sub>10</sub>.

**3.2. Mechanistic Insights into Oxidative Decomposition of *exo*-THDCP.** We can summarize the key experimental results on compositions of products formed from *exo*-THDCP in the presence of O<sub>2</sub> as follows:

- Most of the oxidative decomposition products 2–10 from *exo*-THDCP were C<sub>10</sub> compounds, which were formed independently of its thermal decomposition products 11–17.
- The ratios of products 4 and 2 to all compounds gradually decreased, whereas that of 8 concomitantly increased while conversion of *exo*-THDCP was not changed.

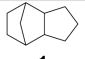
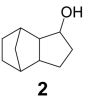
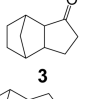
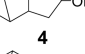
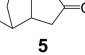
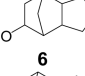
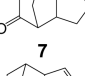
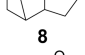
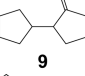
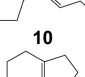
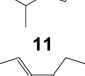



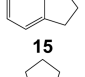
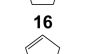
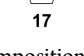
The proposed mechanism for the oxidative decomposition of *exo*-THDCP is illustrated in Figure 3, which explains the experimental results (i) and (ii). *exo*-THDCP **1** is converted to products 2–7 via H abstraction, and products 2 and 4 are then converted to product 8 via dehydration. *exo*-THDCP **1** is also converted to product 9 via H abstraction and C–C cleavage, and product 9 is then converted to product 10 via radical rearrangement and C–C cleavage.<sup>18</sup>

Our proposed mechanism for the oxidative decomposition of *exo*-THDCP (RH<sub>2</sub>) can be summarized as follows:<sup>18,34–39</sup>



Radical (RH·, RHO·, RHO·, R'H·, R'HOO·, and R'HO·) and hydroperoxide (RHOH and R'HOOH) formation steps 1–7 and 11–15 involve H abstraction and radical rearrangement, whereas radical termination (product (RHOH, RO, R, R'O, and R'')) formation) steps 5–8, 10, and 15–17 involve H addition and H abstraction. RH<sub>2</sub> (*exo*-THDCP **1**) is oxidized in step 1, and then converted to RHOH (**2**, **4**, and **6**) in steps 5

Table 1. Products Formed upon Decomposition of *exo*-THDCP in the Absence and Presence of O<sub>2</sub> at 370 °C<sup>a</sup>

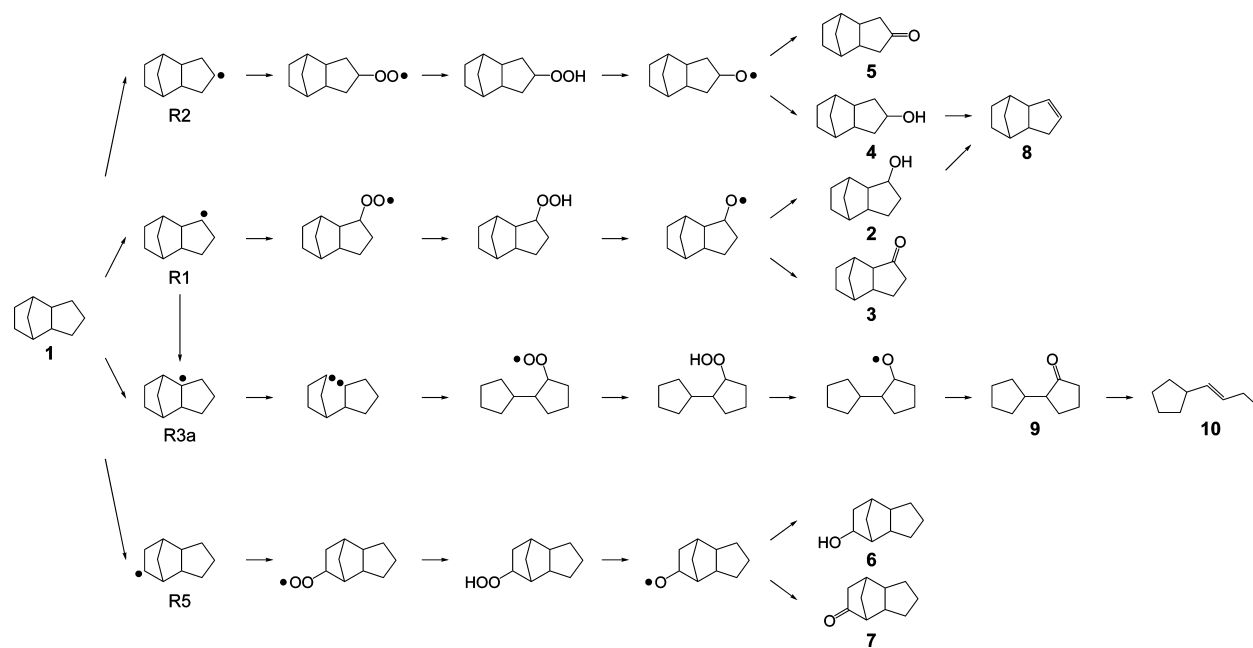
entry	name and abbreviation	structure	formula
1	<i>exo</i> -THDCP		C <sub>10</sub> H <sub>16</sub>
2	THDCP-1-ol		C <sub>10</sub> H <sub>16</sub> O
3	THDCP-1-one		C <sub>10</sub> H <sub>14</sub> O
4	THDCP-2-ol		C <sub>10</sub> H <sub>16</sub> O
5	THDCP-2-one		C <sub>10</sub> H <sub>14</sub> O
6	THDCP-5-ol		C <sub>10</sub> H <sub>16</sub> O
7	THDCP-5-one		C <sub>10</sub> H <sub>14</sub> O
8	THDCP-1-ene		C <sub>10</sub> H <sub>14</sub>
9	2-cyclopentylcyclopentanone (2-CPCPone)		C <sub>10</sub> H <sub>16</sub> O
10	<i>trans</i> -1-butenylcyclopentane (1-BCP)		C <sub>9</sub> H <sub>16</sub>
11	4-methyl-2,3,4,5,6,7-hexahydro-1H-indene (4-MHI)		C <sub>10</sub> H <sub>16</sub>
12	1-cyclopentylcyclopentene (1-CPCP)		C <sub>10</sub> H <sub>16</sub>
13	cyclopentylcyclopentane (CPCP)		C <sub>10</sub> H <sub>18</sub>
14	bicyclopentylidene (BCPI)		C <sub>10</sub> H <sub>16</sub>
15	2,3-dihydro-1-methyl-1H-indene (DMI)		C <sub>10</sub> H <sub>12</sub>
16	cyclopentane		C <sub>5</sub> H <sub>10</sub>
17	cyclopentene		C <sub>5</sub> H <sub>8</sub>

<sup>a</sup>Products from *exo*-THDCP **1** can be classified into oxidative (**2–10**) and thermal (**11–17**) decomposition products as discussed in Section 3.1. Gaseous products H<sub>2</sub> and C<sub>1–4</sub> and unidentified products were omitted.

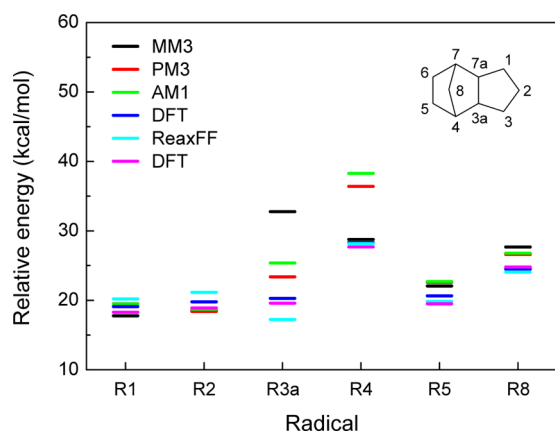
and **6**, RO (**3**, **5**, and **7**) in steps 7 and 8, R (**8**) in step 10, R'O (**9**) in steps 15 and 16, and R'' (**10**) in step 17. Note that H abstraction is the major reaction step in the oxidative decomposition of *exo*-THDCP. H abstraction is also known to be important in the oxidative decomposition of hydrocarbons.<sup>20</sup> To investigate the differences in the product formation kinetics, we carried out molecular and quantum mechanics calculations for intermediates and products formed from *exo*-THDCP.

The relative energies of radicals formed upon H abstraction of *exo*-THDCP are shown in Figure 4. The energies of radicals R1, R2, R5, and R8 (R*n* is denoted for THDCP-R*n* in Figure 4) calculated using MM3, PM3, and AM1 in this work were in

good agreement with those calculated using density functional theory (DFT) and ReaxFF in refs 20 and 21. The average energies of *exo*-THDCP, R1, R2, R3a, R4, R5, and R8 for six calculations were 0.0, 19.1, 19.3, 23.1, 31.3, 21.2, and 25.7 kcal/mol, respectively. Thus, the order of the radical energies were R1 ≈ R2 < R5 < R8 < R4. Note that the order of the product formation rate was 2-ol **4** > 1-ol **2** > 5-ol **6** > 1-one **3** > 2-one **5** > 5-one **7** (see Figure 2; *n*-ol and *n*-one are denoted for THDCP-*n*-ol and THDCP-*n*-one in Table 1, respectively). In addition, 8-ol, 4-ol, 8-one, and 4-one were not detected at all. Both *n*-ol and *n*-one products are formed from the same corresponding R*n* radical upon oxidative decomposition (see



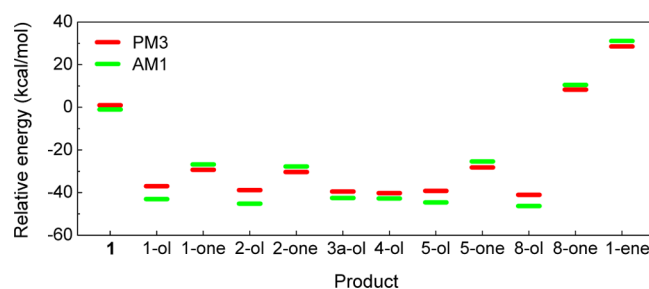
**Figure 3.** Proposed mechanism for the oxidative decomposition of *exo*-THDCP at 200–370 °C. *exo*-THDCP **1** ( $\text{RH}_2$ ) is converted to intermediates and then products 2–10. See the detailed discussion in Section 3.2.  $\text{RH}\cdot$ ,  $\text{RHO}\cdot$ ,  $\text{RHOOH}$ , and  $\text{RHO}\cdot$  are assumed intermediates.<sup>18,34–39</sup> Oxygen molecule ( $\text{O}_2$ ), water ( $\text{H}_2\text{O}$ ), hydroperoxy radical ( $\text{HOO}\cdot$ ), and hydroxyl radical ( $\text{HO}\cdot$ ) described in Section 3.2 are omitted to simplify the mechanism and thereby to clearly show radicals and products formed from *exo*-THDCP. For conversions of radical R1 into R3a ( $R_n$  is denoted for THDCP- $R_n$  in Figure 4), and product 9 into 10 (probably in several steps), see refs 26 and 18, respectively. Such conversions explain the faster formation of 10 compared to 2 (see Figure 2) despite the higher energy of R3a compared to R2 (see Figure 4). For the formation of the diradical from R3a (or 1), see ref 26.



**Figure 4.** Relative energies of radicals formed upon H abstraction of *exo*-THDCP. Here,  $R_n$  is denoted for THDCP- $R_n$ , which is the radical formed from *exo*-THDCP upon H abstraction at its  $C_n$  site (see right top). The energies of radicals  $R_n$  were calculated using MM3, PM3, and AM1 methods as described in Section 2.2. For DFT and ReaxFF data, see refs 20 (blue and cyan) and 21 (magenta).

Figure 3). Thus, the formation of product from a radical with lower energy appears to be faster than that with higher energy.

The relative energies of *exo*-THDCP and its possible oxidative decomposition products are shown in Figure 5. The energies of *exo*-THDCP and its products *n*-ol, *n*-one, and *n*-ene calculated using PM3 were similar to those calculated using AM1. The average energies of *exo*-THDCP, 1-ol, 1-one, 2-ol, 2-one, 3a-ol, 4-ol, 5-ol, 5-one, 8-ol, 8-one, and 1-ene for two calculations were 0.0, −40.0, −28.1, −42.0, −29.0, −41.0, −41.5, −41.9, −26.8, −43.7, 9.4, and 29.8 kcal/mol, respectively. Thus, the average energies of *n*-ol were lower



**Figure 5.** Relative energies of *exo*-THDCP and its possible oxidative decomposition products. Here, *n*-ol, *n*-one, and *n*-ene are denoted for THDCP-*n*-ol, *n*-one, and *n*-ene in Table 1, respectively. Note that 1-ol 2, 1-one 3, 2-ol 4, 2-one 5, 5-ol 6, 5-one 7, and 1-ene 8 were detected products (see Figure 2 and Table 1), whereas 3a-ol, 4-ol, 8-ol, and 8-one were undetected products. The energies of *exo*-THDCP **1** and its products *n*-ol, *n*-one, and *n*-ene were calculated using PM3 and AM1 methods as described in Section 2.2.

than those of *n*-one. In addition, the average energies of 1-ene and 8-one were quite higher than those of the other products. Note that the formation rate of *n*-ol was faster than that of *n*-one (see Figure 2). In addition, 1-ene was formed only at 300 °C or above and 8-one was not detected at 200–370°. Thus, the formation of a product with lower energy appears to be faster than that with higher energy.

#### 4. CONCLUSION

We investigated the decomposition of *exo*-THDCP in the absence and presence of  $\text{O}_2$  at various temperatures. It was found that the oxidative decomposition of *exo*-THDCP occurred independently of its thermal decomposition. We proposed the mechanism for the oxidative decomposition of

*exo*-THDCP, which explains distinct product formation thereupon near and below its thermal decomposition starting temperature. Our proposed mechanism provides a mechanistic framework for further studying the decomposition of *exo*-THDCP in the presence of O<sub>2</sub> at higher temperatures and the role of H donors in lowering its thermal and oxidative decomposition.

## ■ ASSOCIATED CONTENT

### ■ Supporting Information

Figure and tables showing compositions of products and their comparison obtained upon decomposition of *exo*-THDCP in the absence and presence of O<sub>2</sub> at 350 and 370 °C. This material is available free of charge via the Internet at <http://pubs.acs.org>.

## ■ AUTHOR INFORMATION

### Corresponding Author

\*E-mail: kimsh@korea.ac.kr (S.H.K.; phone: (82) 2-3290-3297) and hogyuhan@korea.ac.kr (H.H.; phone: (82) 2-3290-3134).

### Author Contributions

#These two authors contributed equally to this work.

### Notes

The authors declare no competing financial interest.

## ■ ACKNOWLEDGMENTS

This work was supported by the Korea University grant and the KETEP Human Resources Development (No. 2011-4010203050) grant to S.H.K.

## ■ REFERENCES

- (1) Heneghan, S. P.; Zabarnick, S.; Ballal, D. R.; Harrison, W. E., III. JP-8 + 100: The Development of High-Thermal-Stability Jet Fuel. *J. Energy Resour. Technol.* **1996**, *118*, 170–179.
- (2) Maurice, L. Q.; Lander, H.; Edwards, T.; Harrison, W. E., III. Advanced Aviation Fuels: A Look Ahead via a Historical Perspective. *Fuel* **2001**, *80*, 747–756.
- (3) Edwards, T. Liquid Fuels and Propellants for Aerospace Propulsion: 1903–2003. *J. Propul. Power* **2003**, *19*, 1089–1107.
- (4) Edwards, T. Advancements in Gas Turbine Fuels from 1943 to 2005. *J. Eng. Gas Turbines Power* **2007**, *129*, 13–20.
- (5) Burdette, G. W.; Lander, H. R.; McCoy, J. R. High-Energy Fuels for Cruise Missiles. *J. Energy* **1978**, *2*, 289–292.
- (6) Chung, H. S.; Chen, C. S. H.; Kremer, R. A.; Boulton, J. R.; Burdette, G. W. Recent Developments in High-Energy Density Liquid Hydrocarbon Fuels. *Energy Fuels* **1999**, *13*, 641–649.
- (7) Davidson, D. F.; Horning, D. C.; Herbon, J. T.; Hanson, R. K. Shock Tube Measurements of JP-10 Ignition. *Proc. Combust. Inst.* **2000**, *28*, 1687–1692.
- (8) Li, S. C.; Varatharajan, B.; Williams, F. A. Chemistry of JP-10 Ignition. *ALAA J.* **2001**, *39*, 2351–2356.
- (9) Wohlwend, K.; Maurice, L. Q.; Edwards, T.; Striebich, R. C.; Vangsness, M.; Hill, A. S. Thermal Stability of Energetic Hydrocarbon Fuels for Use in Combined Cycle Engines. *J. Propul. Power* **2001**, *17*, 1258–1262.
- (10) Striebich, R. C.; Lawrence, J. Thermal Decomposition of High-Energy Density Materials at High Pressure and Temperature. *J. Anal. Appl. Pyrolysis* **2003**, *70*, 339–352.
- (11) Osmont, A.; Gökalp, I.; Catoire, L. Evaluating Missile Fuels. *Propellants, Explos., Pyrotech.* **2006**, *31*, 343–354.
- (12) Peela, N. R.; Kunzru, D. Thermal Cracking of JP-10: Kinetics and Product Distribution. *J. Anal. Appl. Pyrolysis* **2006**, *76*, 154–160.

- (13) Nakra, S.; Green, R. J.; Anderson, S. L. Thermal Decomposition of JP-10 Studied by Micro-Flowtube Pyrolysis-Mass Spectrometry. *Combust. Flame* **2006**, *144*, 662–674.

- (14) Herbinet, O.; Sirjean, B.; Bounaceur, R.; Fournet, R.; Battin-Leclerc, F.; Scacchi, G.; Marquaire, P.-M. Primary Mechanism of the Thermal Decomposition of Tricyclodecane. *J. Phys. Chem. A* **2006**, *110*, 11298–11314.

- (15) Li, D.; Fang, W.; Xing, Y.; Guo, Y.; Lin, R. Spectroscopic Studies on Thermal-Oxidation Stability of Hydrocarbon Fuels. *Fuel* **2008**, *87*, 3286–3291.

- (16) Xing, Y.; Fang, W.; Xie, W.; Guo, Y.; Lin, R. Thermal Cracking of JP-10 Under Pressure. *Ind. Eng. Chem. Res.* **2008**, *47*, 10034–10040.

- (17) Xie, W.; Fang, W.; Li, D.; Xing, Y.; Guo, Y.; Lin, R. Coking of Model Hydrocarbon Fuels under Supercritical Condition. *Energy Fuels* **2009**, *23*, 2997–3001.

- (18) Xing, Y.; Li, D.; Xie, W.; Fang, W.; Guo, Y.; Lin, R. Catalytic Cracking of Tricyclo[5.2.1.0<sup>2,6</sup>]decane over HZSM-5 Molecular Sieves. *Fuel* **2010**, *89*, 1422–1428.

- (19) Jiao, C. Q.; Ganguly, B. N.; Garscadden, A. Mass Spectrometry Study of Decomposition of *exo*-Tetrahydrodicyclopentadiene by Low-Power, Low-Pressure rf Plasma. *J. Appl. Phys.* **2009**, *105*, 033305.

- (20) Chenoweth, K.; van Duin, A. C. T.; Dasgupta, S.; Goddard, W. A., III. Initiation Mechanisms and Kinetics of Pyrolysis and Combustion of JP-10 Hydrocarbon Jet Fuel. *J. Phys. Chem. A* **2009**, *113*, 1740–1746.

- (21) Hudzik, J. M.; Asatryan, R.; Bozzelli, J. W. Thermochemical Properties of *exo*-Tricyclo[5.2.1.0<sup>2,6</sup>]decane (JP-10 Jet Fuel) and Derived Tricyclodecyl Radicals. *J. Phys. Chem. A* **2010**, *114*, 9545–9553.

- (22) Seiser, R.; Niemann, U.; Seshadri, K. Experimental Study of Combustion of *n*-Decane and JP-10 in Non-Premixed Flows. *Proc. Combust. Inst.* **2011**, *33*, 1045–1052.

- (23) Magoon, G. R.; Aguilera-Iparraguirre, J.; Green, W. H.; Lutz, J. J.; Piecuch, P.; Wong, H.-W.; Oluwole, O. O. Detailed Chemical Kinetic Modeling of JP-10 (*exo*-Tetrahydrodicyclopentadiene) High-Temperature Oxidation: Exploring the Role of Biradical Species in Initial Decomposition Steps. *Int. J. Chem. Kinet.* **2012**, *44*, 179–193.

- (24) Guo, F.; Cheng, X.; Zhang, H. ReaxFF Molecular Dynamics Study of Initial Mechanism of JP-10 Combustion. *Combust. Sci. Technol.* **2012**, *184*, 1233–1243.

- (25) Park, S. H.; Kwon, C. H.; Kim, J.; Chun, B.-H.; Kang, J. W.; Han, J. S.; Jeong, B. H.; Kim, S. H. Thermal Stability and Isomerization Mechanism of *exo*-Tetrahydrodicyclopentadiene: Experimental Study and Molecular Modeling. *Ind. Eng. Chem. Res.* **2010**, *49*, 8319–8324.

- (26) Park, S. H.; Kim, J.; Chun, J. H.; Chung, W.; Lee, C. H.; Chun, B.-H.; Han, J. S.; Jeong, B. H.; Han, H.; Kim, S. H. Mechanistic Insights into Thermal Stability Improvement of *exo*-Tetrahydrodicyclopentadiene by 1,2,3,4-Tetrahydroquinoline. *Ind. Eng. Chem. Res.* **2012**, *51*, 14949–14957.

- (27) Park, S. H.; Kim, J.; Chun, J. H.; Chung, W.; Kim, S. G.; Lee, C. H.; Chun, B.-H.; Han, J. S.; Jeong, B. H.; Han, H.; Kim, S. H. Metal Effects on the Thermal Decomposition of *exo*-Tetrahydrodicyclopentadiene. *Ind. Eng. Chem. Res.* **2013**, *52*, 4395–4400.

- (28) Park, S. H.; Kwon, C. H.; Kim, J.; Chun, J. H.; Chung, W.; Chun, B.-H.; Han, J. S.; Jeong, B. H.; Han, H.; Kim, S. H. Thermal Stability Improvement of *exo*-Tetrahydrodicyclopentadiene by 1,2,3,4-Tetrahydroquinoxaline: Mechanism and Kinetics. *J. Phys. Chem. C* **2013**, *117*, 7399–7407.

- (29) Gasteiger, J. An Algorithm for Estimating Heats of Reaction. *Comput. Chem.* **1978**, *2*, 85–88.

- (30) Allinger, N. L.; Yuh, Y. H.; Lii, J.-H. Molecular Mechanics. The MM3 Force Field for Hydrocarbons. *1. J. Am. Chem. Soc.* **1989**, *111*, 8551–8566.

- (31) Lii, J.-H.; Allinger, N. L. Molecular Mechanics. The MM3 Force Field for Hydrocarbons. 3. The van der Waals' Potentials and Crystal Cata for Aliphatic and Aromatic Hydrocarbons. *J. Am. Chem. Soc.* **1989**, *111*, 8576–8582.

- (32) Stewart, J. J. P. Optimization of Parameters for Semiempirical Methods II. Applications. *J. Comput. Chem.* **1989**, *10*, 221–264.

- (33) Muller, P. Glossary of Terms Used in Physical Organic Chemistry. *Pure Appl. Chem.* **1994**, *66*, 1077–1184.
- (34) Zabarnick, S. Chemical Kinetic Modeling of Jet Fuel Autoxidation and Antioxidant Chemistry. *Ind. Eng. Chem. Res.* **1993**, *32*, 1012–1017.
- (35) Edwards, T.; Zabarnick, S. Supercritical Fuel Deposition Mechanisms. *Ind. Eng. Chem. Res.* **1993**, *32*, 3117–3122.
- (36) Heneghan, S. P.; Zabarnick, S. Oxidation of Jet Fuels and the Formation of Deposits. *Fuel* **1994**, *73*, 35–43.
- (37) Ervin, J. S.; Zabarnick, S. Computational Fluid Dynamics Simulations of Jet Fuel Oxidation Incorporating Pseudo-Detailed Chemical Kinetics. *Energy Fuels* **1998**, *12*, 344–352.
- (38) Zabarnick, S. Pseudo-Detailed Chemical Kinetic Modeling of Antioxidant Chemistry for Jet Fuel Applications. *Energy Fuels* **1998**, *12*, 547–553.
- (39) Pohorecki, R.; Moniuk, W.; Wierzchowski, P. T. Kinetic Model of Uncatalyzed Oxidation of Cyclohexane. *Chem. Eng. Res. Des.* **2009**, *87*, 349–356.